Soils and Foundations 2015;55(5):1181–1195

HOSTED BY

ELSEVIER

CrossMark

The Japanese Geotechnical Society

Soils and Foundations

www.sciencedirect.com
journal homepage: www.elsevier.com/locate/sandf

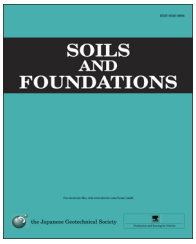

Application of mid-infrared spectroscopy for rapid characterization of key soil properties for engineering land use

B.K. Waruru[a,*], K.D. Shepherd[b], G.M. Ndegwa[c], A. Sila[b], P.T. Kamoni[a]

[a]Kenya Agricultural and Livestock Research Organization (KALRO), P.O. Box 14733-00800, Nairobi, Kenya
[b]World Agroforestry Centre (ICRAF), P.O. Box 30677-00100, Nairobi, Kenya
[c]Jomo Kenyatta University of Agriculture and Technology (JKUAT), P.O. Box 62000-00200, Nairobi, Kenya

Received 25 June 2014; received in revised form 21 April 2015; accepted 22 May 2015
Available online 1 October 2015

Abstract

Methods for rapid and accurate soil tests are needed for the index properties of material attributes commonly applied in civil engineering. We tested the application of mid-infrared (MIR) spectroscopy for the rapid characterization of selected key stability-related soil properties. Two sample sets, representing different soils from across Lake Victoria basin in Kenya, were used for the study: A model calibration set ($n=135$) was obtained following a conditioned Latin hypercube sampling, and a validation set ($n=120$) was obtained from independent sites using a spatially stratified random sampling strategy. Air-dried ground (<0.5 mm) soil was scanned using a high-throughput screening accessory for diffuse reflectance attached to a Fourier transform infrared spectrometer. The soil properties were calibrated to smoothed first derivative MIR spectra using partial least-square regression (PLS), and screening tests were developed for various limitation classes applicable in civil works using the soft independent modeling of class analogy (SIMCA). The hold-out full cross-validation coefficient of determination (r^2) ≥ 0.8 was obtained for the liquid limit (LL), linear shrinkage (LS), coefficient of linear extensibility (COLE), air-dried moisture content, (**W**) and cation exchange capacity (CEC). Further independent validation gave $r^2 \geq 0.73$ and the ratio of prediction deviation (RPD) 4.4–2.1 for LL, LS, COLE, W, CEC, plastic limit (PL), plasticity index (PI), and volumetric shrinkage (VS). The independent validation likelihood ratios for the diagnostic screening tests were: LL > 55%, 4.2; PI > 30%, 2.7; LS > 12%, 2.4; exchangeable sodium (eNa) > 2 cmol (+) kg^{-1}, 2.3; exchangeable sodium percent (ESP) > 10%, 1.8; **W** > 8.3%, 1.6, and Activity number (A) > 1.25 units, 1.5. MIR can provide the rapid assessment of several soil properties that yield stability indices in material testing for engineering land use. Further studies should test the ability of MIR PLS for establishing broader calibrations across more diverse soil types and the direct correlation of MIR to material functional attributes.

Keywords: Mid-infrared spectroscopy; Soil properties; Mixed and separate depth models; Engineering land use; Diagnostic spectral screening

1. Introduction

The increasing demand for quality-intensive soil information, for environmental monitoring, modeling, and civil engineering, calls for the application of the most cost-effective methods of soil data acquisition (Shepherd and Walsh, 2007). Conventional laboratory methods for determining soil properties are often not cost effective as they require a different test for each property and a wide range of equipment and procedures. In addition the methods are often

*Corresponding author. Tel.: +254 02 0729556169.
E-mail addresses: bkwaruru@gmail.com, bkwaruru@yahoo.com (B.K. Waruru), k.shepherd@cgiar.org, shepherd.keith@gmail.com (K.D. Shepherd), georgemndegwa@gmail.com (G.M. Ndegwa), a.sila@cgiar.org (A. Sila), pkamoni@gmail.com (P.T. Kamoni).
Peer review under responsibility of The Japanese Geotechnical Society.

http://dx.doi.org/10.1016/j.sandf.2015.09.018

susceptible to high measurement errors and low precision (Cantarella et al., 2006; Viscarra Rossel and McBratney, 1998). Infrared spectroscopy (IR) has demonstrated several advantages over wet chemistry laboratory methods: (i) IR is rapid (sample preparation and spectral measurement is achieved within 2 min allowing a high throughput of 200–400 samples per day); (ii) a single spectrum integrates information on a number of soil properties, and; (iii) IR measurements are highly precise (Linker, 2012; Shepherd and Walsh, 2002; Viscarra Rossel et al., 2006). For example, Shepherd and Walsh (2003) showed how IR may be used to help improve the accuracy of the reference wet chemistry method. Shepherd et al. (2005) demonstrated that IR was more repeatable than wet chemistry methods by halving the measurement standard deviation (SD). Howari et al. (2002) found a SD of 0.8×10^{-2} nm of spectra readings from soil evaporates and salt crusts, whereas corresponding SD from wet chemistry was 0.32. These properties make spectroscopic analyses combined with multivariate calibration attractive for environmental monitoring and modeling, precision agriculture, and civil engineering (Shepherd and Walsh, 2007; Viscarra Rossel et al., 2008).

The use of diffuse reflectance mid-infrared spectra (MIR) (2500–25000 nm), in combination with partial least-square regression (MIR PLSR), has been investigated in numerous soil studies (Linker, 2012; Shepherd and Walsh, 2007; Viscarra Rossel et al., 2006). However, no studies are available on the application of MIR PLS soil analyses to materials being tested for civil engineering applications. Waruru et al. (2014) demonstrated the satisfactory to weak performance of near-infrared (NIR) (700–2500 nm) for the estimation of soil engineering properties, whereas MIR is reported to be more resourceful than NIR for the prediction of several soil properties (Viscarra Rossel et al., 2006).The question of whether mixed depth (set of samples extracted from different depth intervals) or separate depth (set of samples extracted from one depth interval) MIR PLS models are more effective for the characterization of soil properties has not yet been explored. Few attempts using visible–NIR spectral region (400–2500 nm) (Nanni and Demattê, 2006) have been found, indicating the significant differences in the performance of surface and subsurface sample datasets for the prediction of several soil properties. Moreover, chemometrics- and spectroscopy-based soil calibrations need to be vigorously validated (Brown et al., 2005) to counteract the inherent soil spatial variability (Wang and Cao, 2013) and to ensure geographic model transferability (Reeves, 2010).

Shepherd and Walsh (2002) demonstrated successful diagnostic spectral screening tests for soil properties that were otherwise moderately calibrated to spectra. This suggested that spectral screening would allow the satisfactory classification of soils into basic quality classes. Kariuki et al. (2003) demonstrated strong correlations between infrared spectral parameters in the shortwave infrared (1400–2200 nm) and the established swelling potential indices of the Atterberg limits, CEC, and the coefficient of linear extensibility (COLE) tests. However, no quantification on the predictive performance for spectral screening tests has been reported for soil properties valuable for engineering land use.

The aim of this study is to assess the performance of MIR PLS analyses for the rapid characterization of selected key soil properties valuable for applications in engineering land use. Specifically, the goals of the study are (i) to develop internally validated MIR PLS models for the prediction of several key soil properties for mixed depth and separate depth datasets, and to validate the models using independent sample sets of similar soils; and (ii) to develop independently validated MIR spectra screening tests for various soil limitation classes applicable in civil works. A key question was whether the accuracy of the MIR PLS analyses is sufficient to allow the incorporation of the Atterberg limits and linear shrinkage data into the Africa Soil Information Service (AfSIS) baseline sample of sub-Saharan Africa (Shepherd, 2010; Vågen et al., 2013).

2. Materials and methods

2.1. Selection of sampling sites and field data collection

The study sites fall in an area within Lake Victoria basin (LVB) in the western part of Kenya covering approximately 46,400 km^2 and bound by latitudes 0°7′48″N and 0°24′36″S and longitudes 34°51′E and 35°43′12″E (Fig. 1). Two sets of soil samples were collected following a double-sampling approach (Shepherd and Walsh, 2007). A calibration sample set ($n=135$) was obtained from 46 sites established following a simplified version of the conditioned Latin hypercube sampling (Minasny and McBratney, 2006). At each site in the field, soil samples were collected at three depths (0–20, 20–50, and 50–100 cm) using a Dutch auger. The validation set ($n=120$) was obtained from a larger set ($n=417$) from two different and spatially separated sentinel sites (10×10 km^2 blocks) of lower Nyando (Lny) and Homa Bay (Hby) within LVB. Selection of the sentinel sites, sampling locations, and sample collection in the field followed the land degradation surveillance framework (LDSF) protocol (Vågen et al., 2013). Fig. 2 illustrates the layout and the distribution of the sampling plots in Lny. At each sampling plot in the field, composite samples were taken for three depths: 0–20, 20–50, and 50–100 cm. Prior to the analyses, bulk soil samples were air-dried at 40 °C for two weeks followed by gently crushing the samples and passing them through a 2-mm sieve. Subsamples were used for the analyses.

2.2. Sample preparation and spectral measurement

Spectral measurements for both calibration and validation sets were conducted using a High Throughput Screening device (HTS–XT) attached to a Tensor 27 spectrometer (Bruker Optics, Germany) customized for the MIR spectral range (4000–400 cm^{-1}) (Fig. 3). The measurement protocol elaborated by Terhoeven-Urselmans et al. (2010) was followed. About 5.0 g of each subsample of the air-dry <2 mm soil was ground to <0.5 mm using a natural stone pestle and mortar. The ground sample was thoroughly mixed and homogenized, and approximately 0.5 g was loaded into labeled wells in four replicates in aluminum micro-titer plates consisting of 96 wells (Fig. 4). The first two wells of the plate were used for the standard and blank, respectively, and the first sample was placed in the third well. Scanning was done sequentially for each well. The average reflectance of 32 scans per sample was transformed to absorbance and recorded using the Optics user's software (OPUS) (Bruker Optics, Germany).

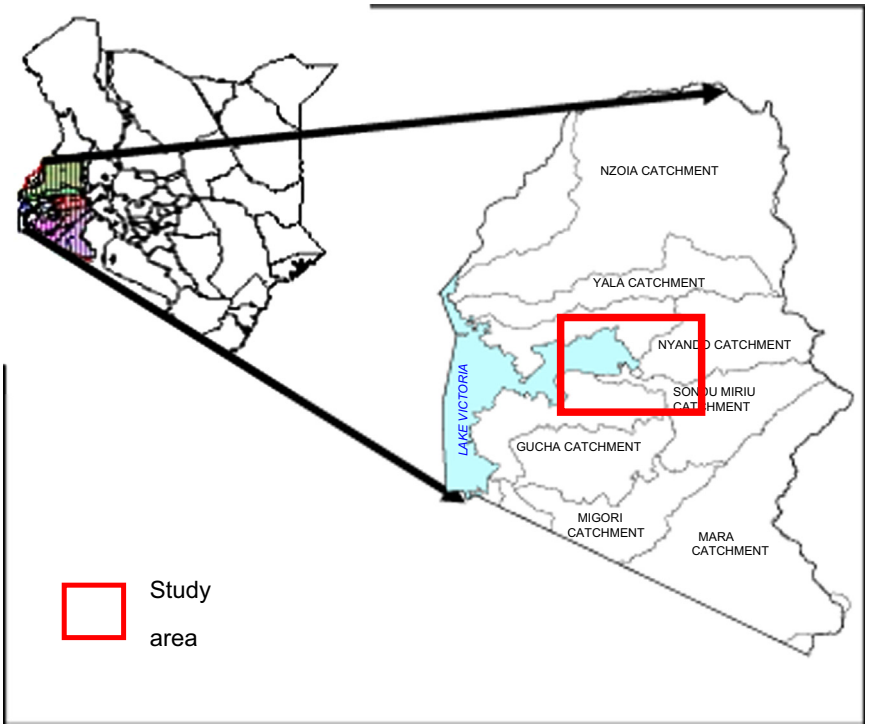

Fig. 1. Map showing the study area within Lake Victoria basin in Kenya (calibration sampling sites were selected from sampled soil profiles to represent different landforms, soil, land covers, and land use within the study area).

2.3. Selection of validation sample set

A principal component analysis (PCA) of the MIR spectra for the combined (Lny and Hby, $n=417$) set was used to select 120 (~25%) representative samples. The scores plotted for the first two principal components (PC1 vs PC2), that together accounted for ***68.1%*** of the total variance, were used to establish the distribution pattern of the soils (Fig. 5). An average of 30 representative samples was selected from each of the 4 quadrants based on the Euclidean distance of the PC space (Naes et al., 2002). Samples with extreme scores in different quadrants (Fig. 5) were also selected to broaden the spectral diversity and corresponding reference validation data range. The selected samples were used to provide reference and spectral values for validation.

2.4. Developing soil property reference data

Soil property data for the calibration and validation of the sample sets was generated using standard laboratory methods, as reported by Shepherd and Walsh (2002) (Table 1).

2.5. Soil Properties

2.5.1. Soil reference and spectra data

Soil property data from calibration samples was sorted into three different datasets: (i) combining samples from the three different depth intervals (0–20, 20–50, and 50–100 cm), (ii) for surface (0–20 cm) samples, and (iii) for subsurface (50–100 cm) samples. A similar sorting was done for the validation samples. For the mixed depth set, this presented a wide range in soil property data, providing a good dataset for subsequent analyses and the development of MIR calibrations. The data range for the validation set fell within the range of the calibration set for all soil properties (except CEC and tClay). The data ranges for the surface and subsurface sets for the validation set were within the corresponding depth range for the calibration set *(data not shown)* for most soil properties (except CEC, tClay and PL). A match between calibration and validation sample datasets is requisite for developing robust MIR PLS models (Terhoeven-Urselmans et al., 2010). Similar absorption patterns were observed for both calibration and validation sets (Fig. 6), which affirmed that both sets belong to the same soil population.

The spectral signatures near 1100–1000 cm^{-1} (from Si–O stretching vibration) and 3690–3620 cm^{-1} (from clay lattice Al-OH vibrations) are associated, for example, with quartz and kaolinite clays, respectively, and bands in the range 3100–2800 cm^{-1} are ascribed to organic components (Nguyen et al., 1991; Viscarra Rossel et al., 2006; 2008) (Fig. 6). Absorbance at these wavebands resonates strongly with reference values of spectrally active soil constituents (including **W**, SOC, and texture parameters), allowing for accurate estimations of the constituents. Soil properties that are spectrally non-responsive (for instance, exchangeable bases and mechanical properties) are predicted through secondary calibrations ascribed to their individual level of association with the active soil constituents (Reeves, 2010).

2.5.2. Reference data distribution

Sodicity indices (eNa, ESP, and Na5), tSa, and PL were highly skewed and natural log (ln) transformation was applied to reduce the skewness. Soil CEC and **W** were slightly skewed and square-root transformation was applied. Texture (tClay and tSi), Atterberg limits

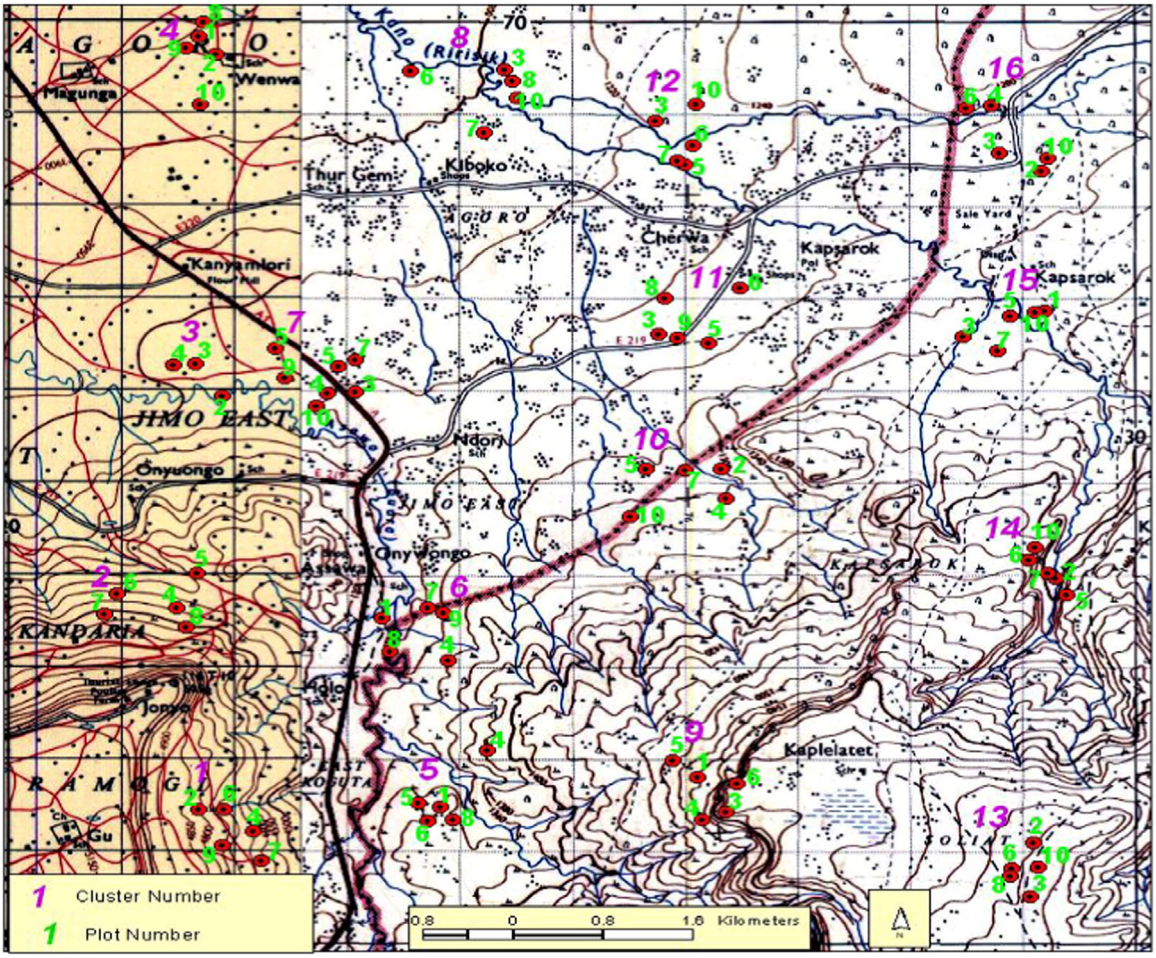

Fig. 2. Sentinel site showing the distribution of clusters and sampling plots (cluster numbers are shown in purple; five priority sampling plots for each cluster are shown in red). (For interpretation of the references to color in this figure legend, the reader is referred to the web version of this article.)

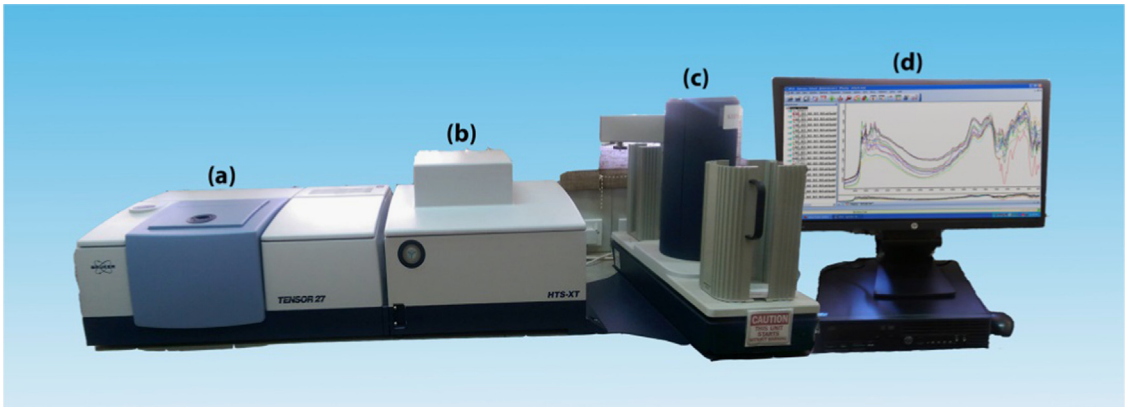

Fig. 3. MIR diffuse reflectance measurement of soil samples showing: (a) Tensor 27® Fourier Transform Infrared (FT-IR) spectrometer; (b) high-throughput screening device (HTS–XT); (c) robotic arm for holding and conveying samples into HTS–XT; and (d) measured soil absorbance spectra.

(LL, PI), LS, and associated COLE, VS, and A approximated a Gaussian distribution and no linearization transformation was used. Fig. 7 illustrates the data distribution for properties in the validation set. The MIR PLS analysis is suboptimal for soil properties with a non-linear data distribution (Linker, 2012).

2.6. Association of soil properties

A pair-wise correlation coefficient (r-value) was used to establish the strength of the linear correlation of the soil properties. Correlations were done using R software version

2.15.1 (R-Development Core Team, 2012). The correlation was considered strong for $r \geq 0.68$, moderate for $0.36 > r \leq 0.67$, and low or weak for $r \leq 0.35$ (Taylor, 1990).

2.7. Calibration of soil properties

The reference soil data and corresponding MIR spectra were preprocessed prior to developing a calibration model for each of the soil properties. The reference data was mean-centered and then standardized (1/SD). The absorbance spectrum for each sample was transformed to the first derivative and then smoothened by applying a smoothing function (Savitzky–Golay filter). The spectral range between 4000 and 600 cm^{-1} (total 1755 wavebands) was selected for the transformed spectra to eliminate wavebands with low signal-to-noise ratios (see Fig. 6). Spectral outliers were checked using the Robust Mahalanobis distance (H) criterion, and samples with $H > 2$ were considered outliers and excluded from the analysis. The transformed MIR wavebands (independent variables) were then calibrated against the preprocessed reference data for each of the soil properties (dependent variables) using partial least-square regression (PLSR) (commonly PLS). Calibrations were evaluated using leave-out-one cross-validation (looCV). Data pretreatment and model calibration were done using The Unscrambler version 9.02 (CAMO technologies, Inc., Woodbridge, NJ). Fig. 8 illustrates the scheme and sequential steps used for development of the calibration models for the soil properties.

Fig. 4. Aluminum plate with sample-filled micro-titer engraved wells.

The coefficient of determination for the measured and predicted values (r^2) and the root mean square error of the cross-validation (RMSECV) were used to evaluate the predictive ability of the models. The RMSECV was calculated as follows:

$$\mathrm{RMSECV} = \left[\sum (y-x)^2/(n-1) \right]^{1/2} \quad (1)$$

where y is the predicted value by the MIR PLS technique for soil properties in the calibration set, x is the reference value for the properties in the calibration set, and n is the total number of calibration samples used. Also used to evaluate the reliability of the calibration models was RPD, the ratio of SD of the measured values in the calibration set to the RMSECV. Calibration models were developed for mixed depth (0–20, 20–50, and 50–100 cm), surface (0–20 cm), and subsurface (50–100 cm) sample datasets.

The rationale and preprocessing of the reference values and the spectral data for PLS modeling has been provided in other works (Naes et al., 2002; CAMO ASA Inc., 1998). Calibration in The Unscrambler has been well elaborated in other studies (Canasveras et al., 2010).

2.8. Calibration independent validation

MIR PLS looCV models for soil properties were further tested using similarly preprocessed reference and MIR data of similar soils from independent sites. The predictive ability of the looCV models

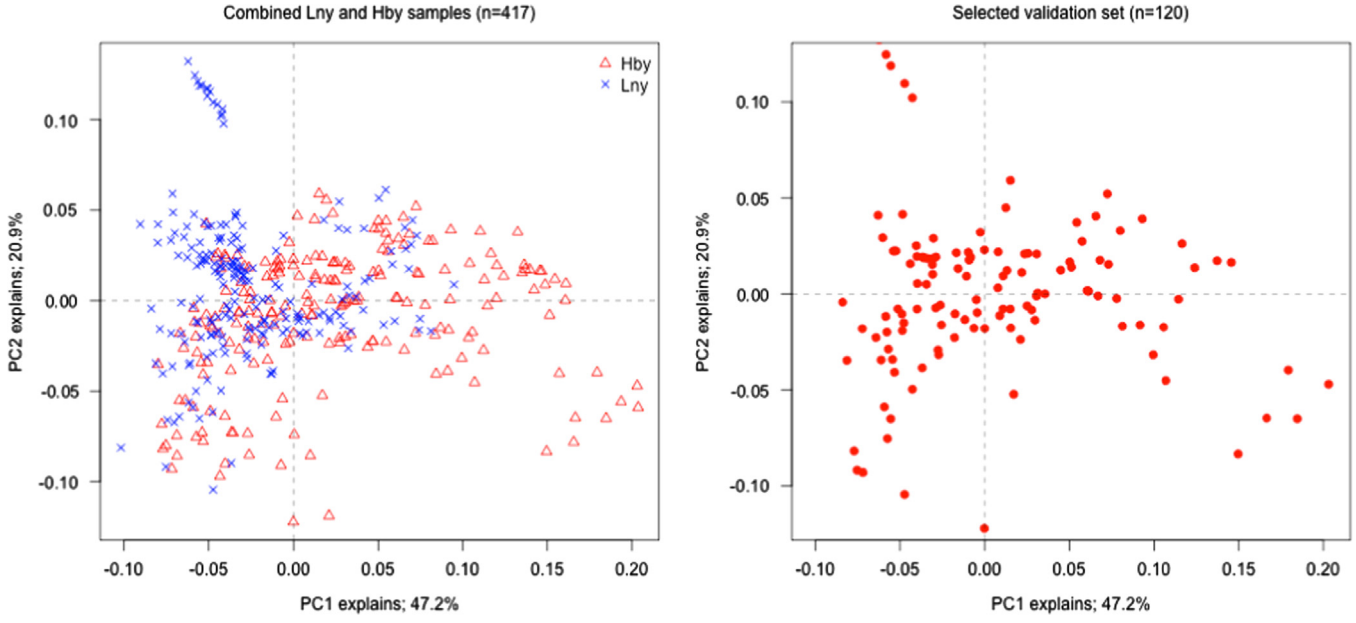

Fig. 5. PCA score plots (PC1 vs PC2) for MIR spectra of combined Lny and Hby ($n=417$ samples) to select 120 samples for model validation (PCA was run in R software version 2.15.1; indicated also is a plot for the distribution of selected validation samples).

Table 1
Soil properties and methods.

Soil property	Method of determination	Reference
Air-dried moisture content (**W**)	Gravimetric (%)	Islam et al. (2003)
Particle-size distribution tClay, tSi, tSa	Hydrometer (%)	Gee and Bauder (1986)
Exchangeable Ca (eCa), Mg (eMg)	1:10 soil-to-1.0 N KCL extraction followed by AAS (cmol(+)kg^{-1})	Shepherd and Walsh (2002)
Exchangeble Na (eNa)	1:10 soil-to-1.0 N KCL extraction followed by AES (cmol(+) kg^{-1})	Shepherd and Walsh (2002)
Exchangeable K (eK)	1:10 soil-to-modified Olsen solution extraction followed by AAS (cmol(+)kg^{-1})	Shepherd and Walsh (2002)
Cation exchange capacity (CEC)	Sum of eCa+eMg+eNa+eK (cmol(+)kg^{-1})	Shepherd and Walsh (2002)
ESP	Ratio [(eNa/CEC)*100] (%)	Viscarra Rossel et al. (2008)
Sodium-ion concentration	1:5 soil-to-water extract read on Na-ion electrode meter (Na5, mg kg^{-1})	Irvine and Reid (2001)
Soil organic carbon (SOC)	Dry combustion using CN analyzer (%)	Viscarra Rossel et al., 2008
Atterberg limits: LL, PL, LS	BSI BS: 1377 (%)	BSI (1975)
Plasticity index (PI)	Numeric difference (PI=LL−PL) (%)	BSI (1975)
Coefficient of extensibility (COLE)	from LS data [(COLE=(Lm−Ld)/Ld)] (unit); where Lm=length moist soil (=140 mm), Ld=length dry soil (140–LS mm)	Igwe (2003)
Volumetric shrinkage (VS)	From COLE data, VS=[(COLE+1)^3−1]*100 (%)	Igwe (2003)
Activity number (A)	A=PI/tClay (%)	Fratta et al. (2007)

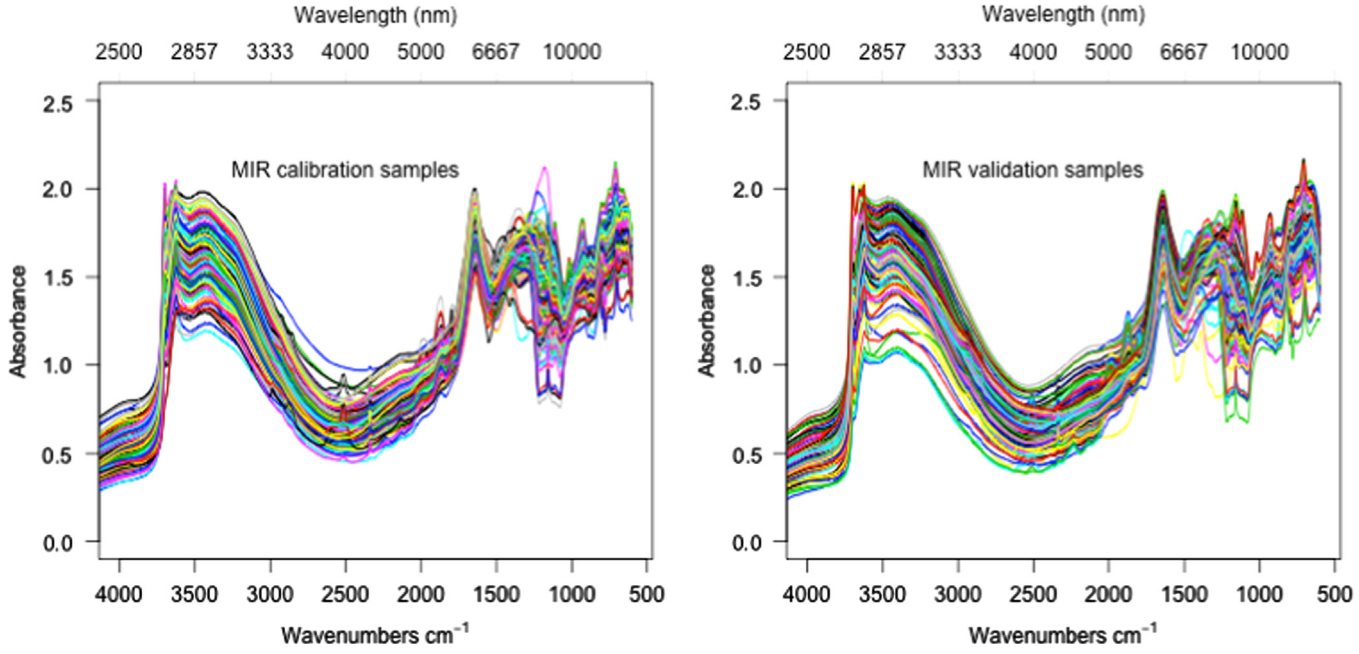

Fig. 6. Mid-infrared absorbance spectra for calibration (n=135) and validation (n=120) of soil samples after removal of the noisy part (< 600 cm^{-1}) of the signal (spectra is shown in both wavenumbers (cm^{-1}) and wavelength (nm) for easy reference, where [(10,000,000/wavenumbers)=wavelength)].

was evaluated by the coefficient of determination for measured and predicted values in the validation set (r^2), the root mean square error of prediction (RMSEP), and the RPD (ratio of SD to RMSEP for validation sample set). The RMSEP was computed using Eq. (1), where y is the predicted value by the MIR PLS looCV model for soil properties in the validation set, x is the reference value for the

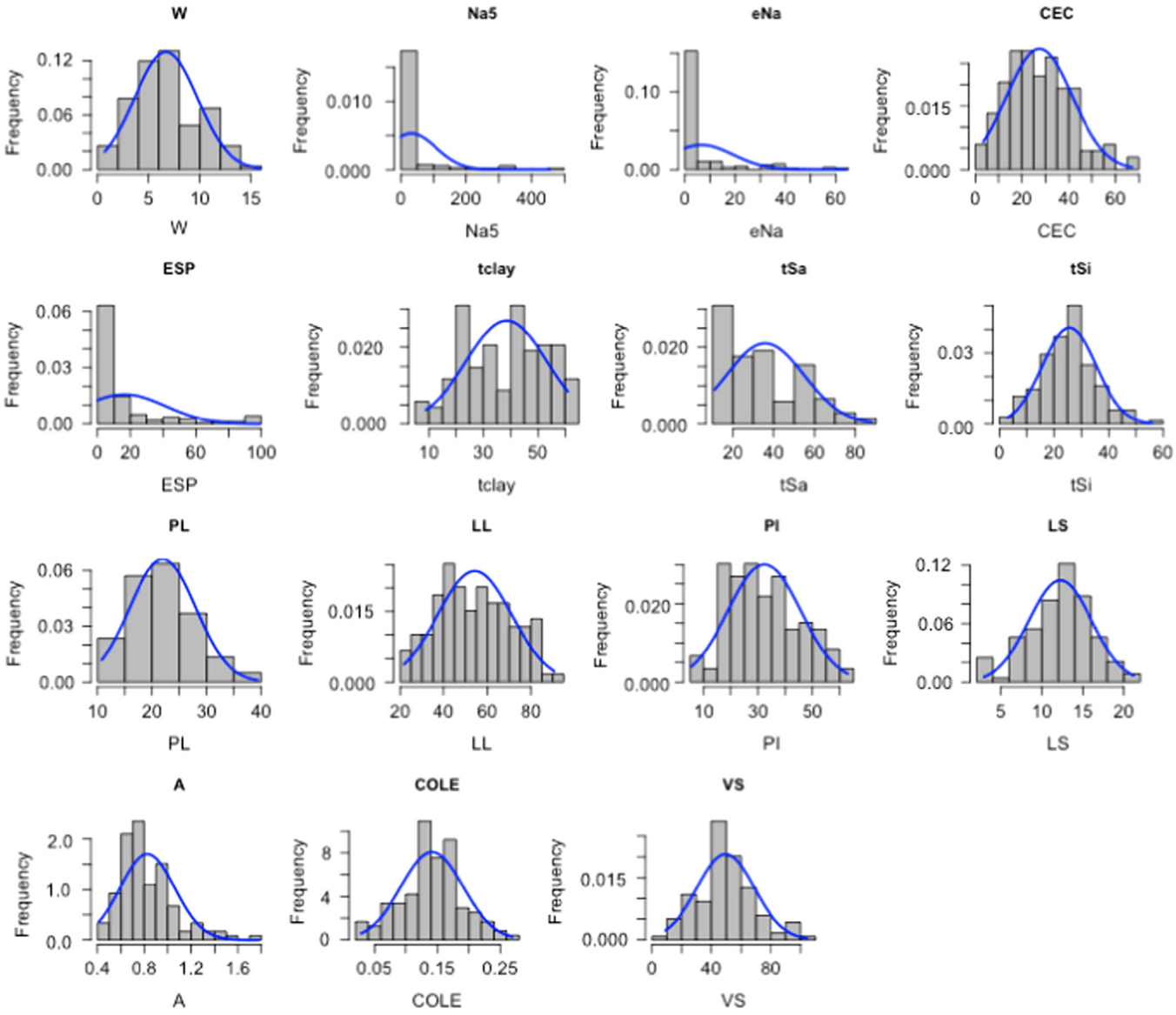

Fig. 7. Data distribution for soil properties from the validation samples.

properties in the validation set, and n is the total number of validation samples used. Predictions were made for mixed depth, surface and subsurface sample datasets.

Calibration and validation statistics (r^2, RMSECV/RMSEP, and RPD) were given for back-transformed data. Good independent predictions were regarded as models having $r^2 > 0.75$ and RPD > 2.0. Satisfactory predictions had r^2 from 0.65 to 0.75 and RPD from 1.4 to 2.0. Predictions below these values were considered to be poor (Terhoeven-Urselmans et al., 2010); however, interpretations were also based on the performance of the spectral diagnostic screening tests.

2.9. Handling outliers

Ten (10) spectral outliers were identified (Robust Mahalanobis distance, $H > 2$) for the mixed depth set from the calibration set. Additionally, one influential outlier (sample with high leverage and high prediction residual) was found for each eNa, ESP, and tSa. Two (2) influential outlier samples were found for Na5. These samples were removed and the model statistics (r^2, RMSECV) were recomputed. Two samples in the validation set presented inadequate soil materials for the determination of **W**. Reference value outliers were defined as samples whose prediction residual (measured- predicted value) was $> 3 \times$ RMSEP (Pirie et al., 2005). Non-plastic (NP) soils and samples with spurious predictions (extremely high or negative predictions) were also considered as reference value outliers and were excluded. The total number of samples identified as reference outliers for the mixed depth validation set were as follows: 2 (ESP, **W**), 3 (eNa, Na5), 4 (CEC), 5 (tClay), 7 (PI), 8 (tSa, LL, PL, COLE, and VS), and 9 (LS, A). These samples were removed and the prediction model statistics (r^2, RMSEP) were recalculated. No reference value outlier was found for tSi for the validation set. Spectral outliers were not checked for separate depth models due to limited sample size ($43 \geq n \geq 38$); however, reference values and influential outliers for both calibration and validation sets were excluded.

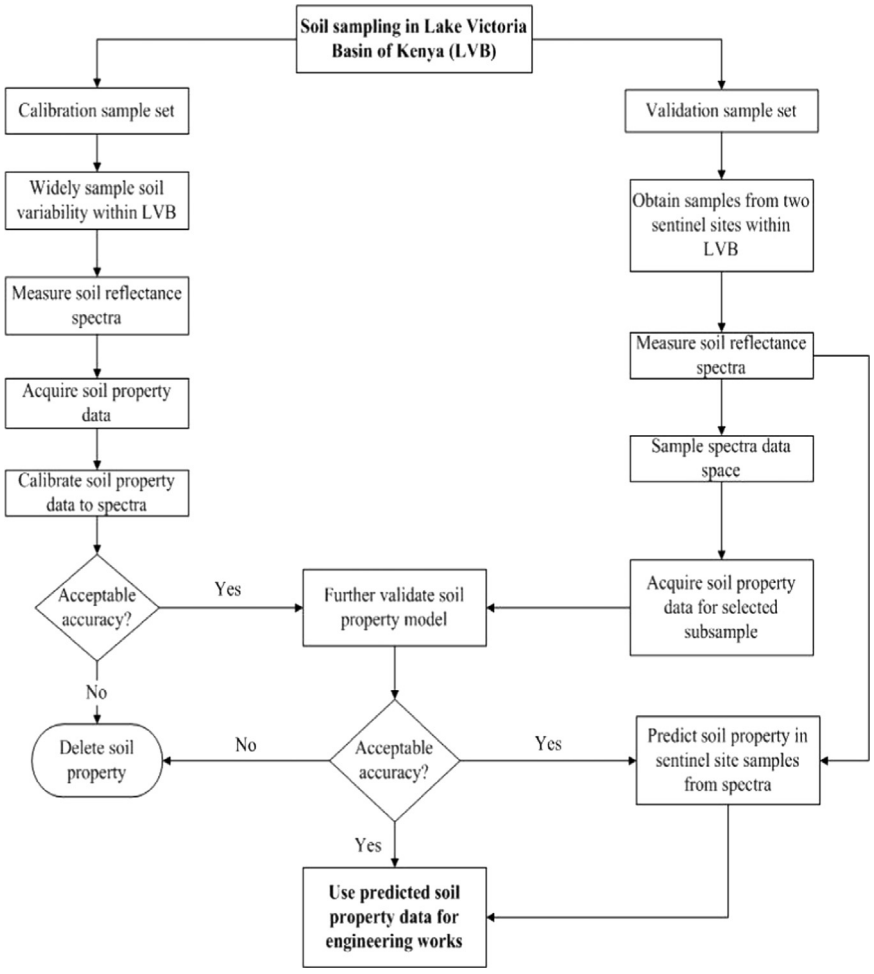

Fig. 8. Scheme for development of MIR-based models for prediction of key soil properties for application in engineering land use.

2.10. Developing soil spectral screening tests

To test the predictive performance of MIR wavebands for the given threshold values of the selected soil properties, a number of screening tests were conducted. The tests were based on commonly used limitation classes that define broad categories of soils in terms of their predicted behavior, and for earthworks recommendations (for instance, small dams, untreated roads, and small buildings) (Hazelton and Murphy, 2007). Soils were classified either as normal ('stable') or abnormal ('unstable') based on a cut-off value defined by the class limit (Table 2). Reference data values for Na5 at 25th and 75th percentiles (Shepherd and Walsh, 2002) were used to define the stable and unstable cut-offs, respectively. Classification models using SIMCA (soft independent modeling of class analogy), implemented in R (rrcovHD package) (Todorov, 2013), were used to develop cross-validated calibrations for each screening test with the 1755 MIR wavebands as dependent variables. The best model-comparing models based on 2 through 10 principal components (PCs) were selected. The predictive ability of the resulting models was further tested using similarly preprocessed MIR spectral wavebands for the independent sample set. The predictive performance was assessed using the sensitivity (percentage of abnormal (unstable) cases correctly predicted), specificity (percentage of normal (stable) cases correctly predicted), and positive likelihood ratio [percentage sensitivity/[100 − percentage specificity] tests, which indicate the value of the test for increasing certainty about a positive diagnosis (Shepherd and Walsh, 2002).

The success of spectral screening tests depends not only on the performance of the diagnostic tests (sensitivity, specificity, and likelihood ratio), but also on the prevalence of the abnormal cases in the population studied (Shepherd and Walsh, 2002). The prevalence of abnormal cases in the validation set was computed as (100 × [abnormal cases/total samples in validation set]).

3. Results and discussion

3.1. Association of soil properties

Spectrally featureless soil properties, including sodicity indices (eNa, ESP, and Na5), CEC, and mechanical properties (LL, PL, PI, LS, COLE, VS, and A) (secondary properties) are calibrated to reflectance spectra via secondary or surrogate calibrations, occasioned by their individual association with spectrally active soil constituents including **W**, SOC, and clay mineralogy (reflected by tClay) (Linker, 2012; Reeves, 2010). Table 3 presents the association (r-value) of the soil properties.

Table 2
Definition of soil stability screening tests.

Soil test	*Class limit*[a]	*Category*	*Interpretation*
eNa, cmol(+)/kg	< 1	stable	no spontaneous dispersion; low piping and metastable collapse hazard
eNa, cmol(+)/kg	> 2	unstable	spontaneous dispersion; high piping and metastable collapse hazard
ESP, %	< 6	stable	no spontaneous dispersion; low piping and metastable collapse hazard
ESP, %	> 10	unstable	spontaneous dispersion; serious piping and failures of earth dams
Na5, mg/kg	< 1.9	stable	no spontaneous dispersion; low piping and metastable collapse hazard
Na5, mg/kg	> 17.8	unstable	spontaneous dispersion; high piping and metastable collapse hazard
LL, %	< 45	stable	low compressibility; low shrink-swell potential
LL, %	> 55	unstable	high compressibility; high shrink-swell potential
PI, %	< 15	stable	low compressibility; small surface movement; no limitations
PI, %	> 30	unstable	places limitations for earthworks and foundations
LS, %	< 5	stable	non expansive; no limitations
LS, %	> 12	unstable	expansive; places limitations for earthworks and foundations
COLE, unit	< 0.03	stable	non-expansive; low soil volume-change potential
COLE, unit	> 0.06	unstable	expansive; high soil volume-change potential
VS, %	< 20	stable	low shrink-swell hazard; no limitation
VS, %	> 30	unstable	high shrink-swell; places limitation for earthworks and foundation
A, unit	< 0.75	stable	low shrink-swell potential; chemically inactive (1:1 lattice clays)
A, unit	> 1.25	unstable	high shrink-swell potential; active (2:1 lattice clays)

[a]Definition of class limits and stability category interpretation are for illustrative purposes only; the limitation classes for LL, PI, LS, COLE, and VS assume well-graded soil where samples are passed through a 425 μm sieve screen (Hazelton and Murphy, 2007).

Table 3
Pair-wise correlation coefficient (*r*-value) of soil properties.

W	**Na5**	**eNa**	**CEC**	**ESP**	**tclay**	**tSa**	**tSi**	**PL**	**LL**	**PI**	**LS**	**A**	**COLE**	**VS**	
1.00	0.05	0.08	0.72	0.00	0.70	−0.68	0.26	0.71	0.91	0.87	0.80	0.51	0.80	0.80	**W**
	1.00	0.87	0.59	0.81	0.06	−0.07	0.04	−0.02	0.07	0.10	0.11	0.13	0.12	0.13	**Na5**
		1.00	0.69	0.95	0.08	−0.10	0.08	−0.01	0.05	0.07	0.06	0.10	0.07	0.07	**eNa**
			1.00	0.60	0.51	−0.54	0.28	0.39	0.62	0.64	0.56	0.45	0.57	0.57	**CEC**
				1.00	−0.01	−0.03	0.07	−0.05	−0.05	−0.04	−0.06	0.09	−0.06	−0.06	**ESP**
					1.00	−0.86	0.15	0.57	0.79	0.78	0.72	0.02	0.71	0.69	**tclay**
						1.00	−0.64	−0.58	−0.75	−0.72	−0.72	−0.17	−0.70	−0.67	**tSa**
							1.00	0.28	0.27	0.23	0.31	0.29	0.29	0.27	**tSi**
								1.00	0.78	0.55	0.65	0.34	0.64	0.62	**PL**
									1.00	0.95	0.91	0.55	0.90	0.89	**LL**
										1.00	0.89	0.58	0.89	0.89	**PI**
											1.00	0.58	1.00	0.99	**LS**
												1.00	0.58	0.58	**Ac**
													1.00	1.00	**COLE**
														1.00	**VS**

3.2. Calibration of soil properties

Table 4 presents the model performance (r^2, RMSECV, and RPD) of the MIR PLS prediction of the soil properties for the mixed and separate depth datasets at the calibration stage.

3.2.1. Mixed depth models

A high looCV prediction performance was observed for **W**, CEC, LL, LS, and tSa ($r^2 = 0.90 - 0.72$; RPD = 3.2 − 2.1) (Table 4). The excellent prediction of **W** was attributed to the high resonance of the **W** values with strong moisture absorption features in the MIR region. The high CEC prediction was ascribed to the high association of CEC with **W** (Table 3). The satisfactory prediction of tSa was a result of the high resonance of the tSa values to the intense absorption features of quartz (see Fig. 6), and the strong to moderate association with **W** and tClay (Table 3).

The high prediction of LL and LS (Table 4) was attributed to the high covariance of these properties with spectrally active **W** and tClay (Table 3). A moderate performance was observed for PL, PI, COLE, VS, tClay, and Na5 ($r^2 = 0.7 - 0.6$, RPD = 1.9 − 1.6) (Table 4). The MIR PLS was poor ($r^2 < 0.5$, RPD = 1.5 − 1.2) for the prediction of ESP, tSi, and A (Table 4), attributed to the moderate to poor correlation of the properties with **W** and tClay (Table 3), and to the low quality reference data (that is, tSi and A). Reference values for tSi and A are associated, for example, with the propagation of errors in the determination of tSa

Table 4
Prediction ability of MIR PLS for mixed and separate depth datasets of soil properties at calibration stage.

Soil test	*Mixed depth (0–20, 20–50, 50–100 cm) set*			*Surface (0–20 cm) set*			*Subsurface (50–100 cm) set*		
	r^2	*RMSECV*	*RPD*	r^2	*RMSECV*	*RPD*	r^2	*RMSECV*	*RPD*
eNa	0.55	24.34	0.52	0.39[a]	5.90	1.27	0.40	8.54	1.66
ESP	0.43[a]	17.01	1.48	0.40	15.63	1.28	0.27	20.03	1.36
Na5	0.55	46.65	1.62	0.62	32.70	1.39	0.69[a]	25.00	3.46
CEC	0.87	5.00	2.81	0.88[a]	3.83	2.86	0.81	6.84	2.32
tSa	0.74[a]	9.17	2.07	0.71	12.87	1.54	0.68	10.67	1.73
tSi	0.33	8.02	1.22	0.46[a]	8.16	1.36	0.28	7.83	1.13
tClay	0.60[a]	8.70	1.70	0.56	10.20	1.47	0.52	10.34	1.43
LL	0.85[a]	6.60	2.84	0.86[a]	7.03	2.68	0.84	6.92	2.81
PL	0.62	3.67	1.87	0.70[a]	3.38	2.05	0.62	3.92	1.85
PI	0.62	7.90	1.78	0.68[a]	7.44	1.79	0.53	9.23	1.57
LS	0.72	2.01	2.10	0.79[a]	1.79	2.38	0.62	2.09	2.05
COLE	0.67	0.03	1.85	0.80[a]	0.02	2.17	0.53	0.03	1.47
VS	0.61	11.70	1.76	0.73[a]	10.53	1.90	0.52	13.53	1.57
A	0.37[a]	0.19	1.38	0.25	0.21	1.29	0.09	0.21	1.21
W	0.90	0.96	3.21	0.93	0.82	3.78	0.94[a]	0.75	3.89

[a]The best correlation for each soil test across the three datasets is marked.

and tClay (Reeves, 2010) and tClay and PI (Fratta et al., 2007), respectively.

3.2.2. Separate depth models

The surface (0–20 cm) models were superior over the corresponding mixed depth models for Na5, tSi, LL, PL, PI, LS, COLE, VS, and **W** (Table 4). Notably, the surface models were superior over the mixed depth models for all mechanical properties (except A) (Table 4). The subsurface (50–100 cm) models were superior over the mixed depth models for **W** and Na5 (Table 4). The higher levels and wider range in soil chromophores (**W** and SOC) for the surface soils could partly explain the better correlation of spectra with the secondary properties.

The looCV testing provides a good indicator of the robustness of a model (Canasveras et al., 2010); however, this validation strategy could overestimate the predictive performance (Brown et al., 2005), since samples from the same set are used for calibration and validation. The robusticity of the looCV models of the soil properties for mixed- and separate-depths datasets were, therefore, further tested using datasets for similar soils from independent sites.

3.3. Calibration-independent validation

Table 5 presents the model performance (r^2, RMSEP, and RPD) for the MIR PLS prediction of soil properties for mixed and separate depth datasets at the validation stage.

3.3.1. Mixed depth models

The observed poor estimation of sodicity indices ($r^2 \leq 0.45$, RPD = 1.3–0.8) (Table 5) was attributed to the surrogate nature of the calibration (Reeves, 2010) and the poor correlation of the indices with **W** and tClay. Predictions of Na5 and eNa were similar (Table 5); the two indices were also very strongly correlated (Table 3), suggesting that Na5 could provide an excellent surrogate for eNa.

The excellent prediction of CEC (Table 5; Fig. 9(j)) was attributed to the robust moderate to strong association of CEC with **W** and tClay. The estimates of tClay were modest, whereas the tSa model indicated significant degradation (Table 5; Fig. 9(g) and (h)), affirming that the MIR calibration of tSa is surrogate (Terhoeven-Urselmans et al., 2010). The poor prediction of tSi was attributed to the low quality reference values from the reference method.

The perfect estimation of **W** (Table 5; Fig. 9(i)) is a reflection of the robust resonance of soil moisture with characteristic intense water absorption bands in the MIR region. The high performance of the predictions for LL, PI, LS, COLE, and VS (Table 5; Fig. 9(a), (c), (d), (e), and (f)), respectively, could partly be attributed to the robust covariance of the properties with **W** also in the validation set. Notably, the properties indicated a strong correlation with **W** and tClay ($r \geq 0.7$) (Table 3). Air-dried **W** is an indicator of the clay content and the mineralogy, which directly determine most engineering properties. The content of soil organic matter also affects the air-dried moisture retention, which may also influence the engineering properties. Probably aquaphotomics (water-light interactions), attributed to Stenberg (2010), was also partly responsible for the robust performance. The prediction of PL (Table 5; Fig. 9(b)) was less robust, however, due to the low quality reference values (Waruru et al., 2014) and also to the moderate association of PL with tClay (Table 3).

Janik et al. (1998) reported $r^2 = 0.70$, 0.83, 0.90 for the MIR prediction of soil **W** at air-dried, (−) 10 kPa, and (−) 30 kPa moisture, respectively. This suggested improved prediction performance at a standardized moisture content and with increasing suction. Janik et al. (2007) also found an improved performance for the MIR PLS analyses of the moisture retained at (−)1500 kPa compared with the performance for the moisture retained at (−) 10 kPa ($r^2 = 0.72$ vs 0.54), for the reason that **W** at higher suction is better standardized with less variation for different samples in the set than at lower suction. Less variation in the **W** reference values for different samples results in higher resonance with spectra and better-fitting models (Mouazen et al., 2006). Presumably a similar

Table 5
Prediction ability of MIR PLS looCV models for mixed and separate depth sample datasets for soil properties at validation stage.

Soil test	*Mixed depth (0–20, 20–50, 50–100 cm) set*			*Surface (0–20 cm) set*			*Subsurface (50–100 cm) set*		
	r^2	*RMSEP*	*RPD*	r^2	*RMSEP*	*RPD*	r^2	*RMSEP*	*RPD*
eNa	0.45	7.79	1.19	0.43	2.69[a]	1.20	0.54	14.39	0.85
ESP	0.44	22.51	0.76	0.38	8.12[a]	1.12	0.35	41.76	0.52
Na5	0.40	36.33	1.28	0.28	13.90[a]	0.83	0.36	55.99	1.09
CEC	0.89	5.24	3.17	0.83	5.38	2.18	0.92	5.08[a]	3.78
tSa	0.45	14.29[a]	1.34	0.59	19.01	0.95	0.43	19.52	1.10
tSi	0.28	7.95	0.99	0.51	5.74[a]	1.40	0.39	8.77	0.91
tClay	0.61	13.27[a]	1.28	0.58	12.67	1.20	0.47	15.94	1.16
LL	0.82	8.70	2.55	0.75	8.26	1.98	0.86	9.39[a]	2.70
PL	0.52	4.31	1.85	0.35	4.91	1.48	0.76	3.04[a]	2.91
PI	0.72	8.17[a]	1.97	0.61	6.74	1.74	0.74	8.80[a]	2.06
LS	0.78	1.91	2.47	0.72	2.21	1.81	0.76	1.85[a]	2.79
COLE	0.76	0.03[a]	2.31	0.73	0.03	1.79	0.76	0.03[a]	2.40
VS	0.73	10.87[b]	2.08	0.70	10.98	1.76	0.68	11.96	2.08
A	0.23	0.19	1.61	0.04	0.29	1.10	0.35	0.20[a]	1.52
W	0.93	0.86	3.83	0.94	0.67	4.13	0.95	0.81[a]	4.38

[a]The best prediction for each soil test across the three datasets is marked.

mechanism could partly explain the improved performance for the mechanical properties with moisture standardized at LL.

3.3.2. Separate depth models

Surface and subsurface models for **W** and tSi were superior over the corresponding mixed depth models (Table 5). The surface model for tSa was more robust than the corresponding mixed depth model (Table 5). The subsurface models were more robust than the mixed depth models for eNa, CEC, LL, PL, PI, and A (Table 5). Notably, all the mechanical properties (except VS) were better independently predicted for the subsurface than for the surface datasets, and for the mixed depth set (except for LS and VS) (Table 5). This was probably due to more influence of the texture (tClay) (more homogeneous particle-size distribution and less spectral absorption feature distortion by **W** and SOC) for the subsurface than the surface sets. These observations also suggest the need for assessing separately the surface and subsurface horizon models for a more effective quality assessment of the profile of Base, Sub-base, or Sub-grade *in situ* material.

3.4. MIR PLS reliability and fitness for purpose

Based on the overall model performance rating proposed by Terhoeven-Urselmans et al. (2010), good independent predictions were obtained for CEC, LL, LS, COLE, and **W** ($r^2=0.93-0.78$, RPD$=3.8-2.3$); satisfactory predictions for PI and VS ($r^2=0.7$, RPD$=2.0$); whereas predictions for sodicity indices (eNa, ESP, and Na5), texture (tSa, tSi, and tClay), and mechanical properties (PL and A) were considered poor ($r^2=0.61-0.23$, RPD$=1.3-0.8$) for the mixed depth datasets. The poor models for PL and A, however, were reliable with RPD 1.9 and 1.6, respectively, suggesting that with better quality reference data, the model performance could be improved. In addition, for modest RPD values between 1.5 and 1.69, for the prediction of soil properties, the spectral based predictors are useful for screening purposes, such as discriminating between low and high quality classes (Canasveras et al., 2010).

Ultimately, the key criterion for judging the acceptable prediction accuracy and utility of soil MIR PLS analysis is the fitness for purpose. For rapid geotechnical preliminary site investigations, it is often sufficient to classify a soil with respect to a limitation class value, rather than needing a precise estimate of a soil property (Hazelton and Murphy, 2007). This allows for the making of management decisions (site is stable or unstable), especially for earthworks recommendations (small dams, untreated roads, and small buildings), typical for farm situations where the consequences of failure are lesser (for instance, higher susceptibility to tunneling or piping failure and loss of water) or where the consequences of failure are greater (damage to roads or buildings, or loss of life), for which more rigorous engineering conditions are required (Hazelton and Murphy, 2007). Diagnostic spectral screening tests were developed for limitation classes for selected soil properties.

3.5. Prediction of soil limitation classes

A reasonable predictive performance was achieved for the selected soil spectral screening tests for the independent set (Table 6).

The prediction of the unstable (abnormal) category was, for example, very high for all soil tests (except A) with test sensitivity 71–100%. Test specificity (stable category) ranged from 58% to 100% for eNa, ESP, LL, and A. Even where the MIR PLS calibration was poor (for instance, sodicity indices), spectra screening tests gave good results (sensitivity $>80\%$) (Table 6). This means that the relationship between spectra and the indices values is still strong enough to permit reasonable discrimination of stable and unstable categories. The observed poor prediction of the unstable category, based on A (sensitivity 6%), was attributed to the low prevalence of the unstable category (Table 6) (Shepherd and Walsh, 2002).The range in positive LHR (4.0–2.0) is modest (for instance, Shepherd and Walsh (2002) found LHR 2.7–11.4 for soil fertility screening tests); however, it demonstrates increasing probability of the occurrence of unstable soils.

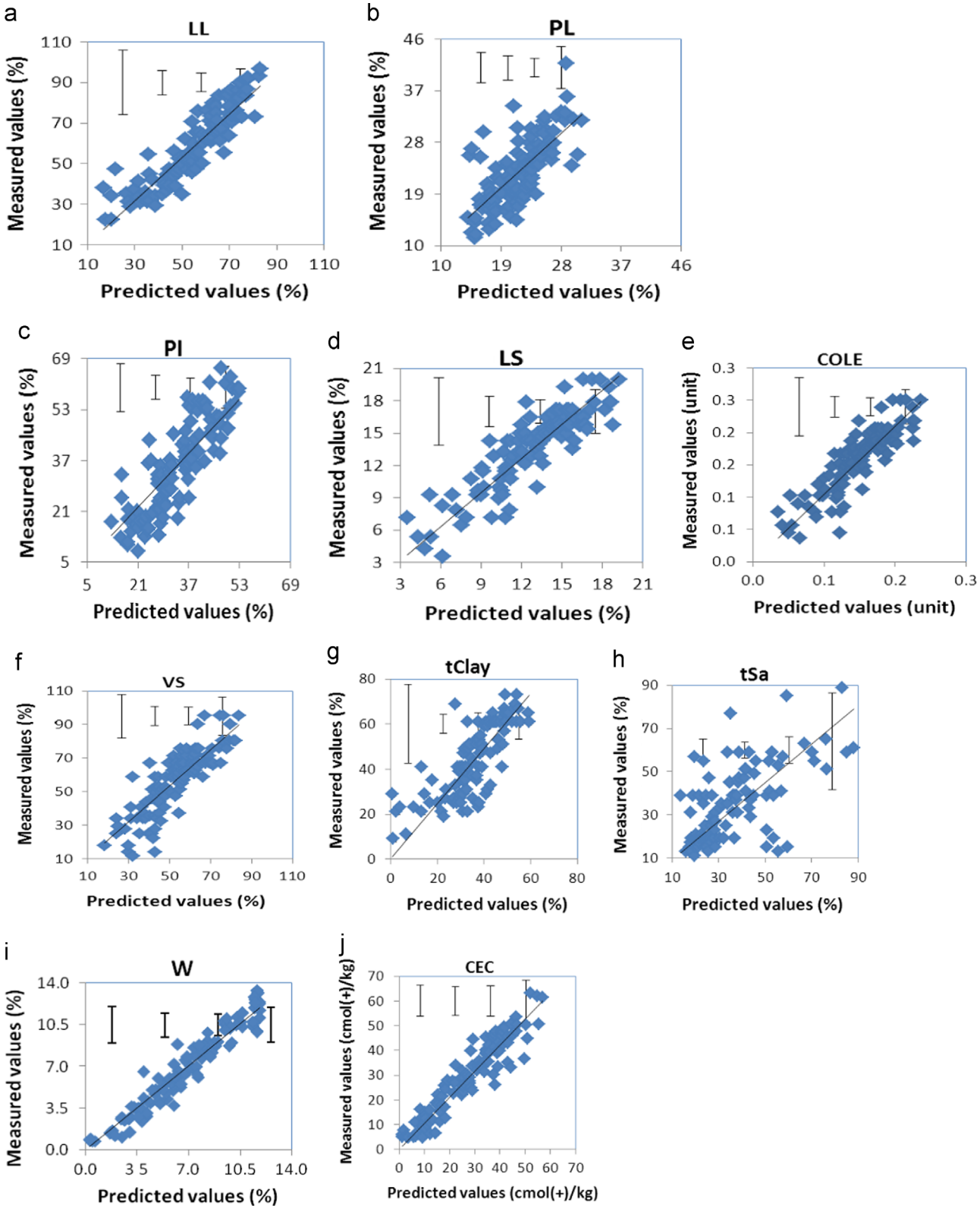

Fig. 9. Scatterplot for measured vs predicted values of selected soil properties for mixed depth data sets (indicated for each plot is also the target (1:1) regression line and standard error bars for quartile data sets).

3.6. Implication for engineering land use

?tlsb -0.015w?>Good to satisfactory MIR PLS looCV predictions were attained for Na5, CEC, tSa, LL, PL, PI, LS, COLE, VS, and **W** ($r^2 = 0.94 - 0.68$, RPD $= 3.9 - 1.8$) (the best performance for each soil test across the three different datasets (mixed, surface, and subsurface) of the calibration set (Table 4)). This suggested that MIR analyses for the

characterization of key soil properties valuable for engineering land use are, in principle, feasible (Reeves, 2010). Further validation of the looCV models indicated that the MIR PLS analysis could achieve very robust predictions for **W**, CEC, LL, PL, LS, and COLE ($r^2=0.95-0.76$, RPD$=4.4-2.4$), and modest but very reliable predictions for PI and VS ($r^2=0.73$, RPD$=2.1$) (the best performance for each soil test across the three different datasets) (Table 5) for independent sets. This could be important because LL, CEC, COLE, and VS are key for developing expansive soil indices for rating shrink-swell potential (Kariuki and van Der Meer, in press; Thomas et al., 2000), whereas the PI is key for assessing piping hazards and soil suitability for bases, subbases, and subgrade for earthworks and foundations for the construction of small buildings (Hazelton and Murphy, 2007).

The reasonable performance observed for the screening tests (sensitivity $\geq 86\%$) will enable rapid and accurate discrimination of materials into 'stable/unstable' categories, with implications for efficient and effective preliminary geotechnical site investigations, especially where large sample sizes are involved.

Separate depth MIR looCV models were more robust than the mixed depth set. Separate depth calibrations would provide more effective quality assessments of the profiles of Base, Subbase, or Sub-grade *in situ* material, critical also for the rapid assessment of materials for borrow pit sites. Recent advances in infrared technology (Ben Dor et al., 2008), suggest the potential for interval-depth MIR spectral data collection in situ. Separate depth models were based, however, on a small sample size ($35 \leq n \leq 46$) and further studies using larger sets are needed to improve on the reliability.

This study demonstrated the great potential of MIR PLS for the rapid characterization of several soil properties commonly employed or that could be employed for engineering land use. Using MIR PLS, several properties can be determined from a single spectrum, which greatly reduces the cost of the analysis compared to conventional laboratory techniques; the measurement is very rapid so that a large number of samples can be easily screened and measurements could be conducted "on-site". The double-sampling approach allows for the prediction of the soil properties at sentinel sites. The predicted values could be combined with remote sensing data in a geographic information system (GIS) environment leading to the spatial mapping of the properties. This has implications for rapid and effective large area preliminary site investigations for civil works.

Table 6
Prediction of soil limitation class tests for selected properties from MIR diffuse reflectance spectra using SIMCA for independent validation datasets.

Soil test	Sensitivity[a]	Specificity[b]	N_{norm}[c]	N_{abn}[d]	LHR[e]	$Prev_{abn}$
eNa < 1.0, cmol (+)/kg	87	70	48	72	2.9	
eNa > 2.0, cmol (+)/kg	86	63	55	65	2.3	54
ESP < 6, %	86	58	50	70	2.1	
ESP > 10, %	81	54	54	66	1.8	55
Na5 < 1.9, mg/kg	88	39	42	78	1.4	
Na5 > 17.8, mg/kg	71	60	61	59	1.8	49
LL < 45, %	99	65	35	84	2.8	
LL > 55, %	98	77	54	65	4.2	55
PI < 15, %	89	ND	13	106	N/A	
PI > 30, %	98	64	48	71	2.7	60
LS < 5, %	92	ND	35	84	N/A	
LS > 12, %	100	58	54	65	2.4	67
COLE < 0.03, unit	98	8	6	113	1.1	
COLE > 0.06, unit	91	ND	11	108	N/A	91
VS < 20, %	91	ND	11	108	N/A	
VS > 30, %	86	100	19	100	ND	84
A < 0.75, unit	51	100	54	55	ND	
A > 1.25, uint	6	96	113	6	1.5	5

$Prev_{abn}$ – prevalence of abnormal cases.
ND – not determined (#DIV/0!).
N/A – not applicable (#VALUE!).
[a]Percentage of abnormal (unstable) cases correctly classified (e.g., percentage of cases with LL > 55%).
[b]Percentage of normal (stable) cases correctly classified (e.g., percentage of cases with LL ≤ 45%).
[c]Number of normal (stable) cases in the validation set.
[d]Number of abnormal (unstable) cases in the validation set.
[e]Likelihood ratio (LHR)=(percentage sensitivity/[100 − percentage specificity]).

4. Conclusion and recommendations

The application of DRIFT MIR combined with PLS was tested for the rapid characterization of soil sodicity indices, cation exchange capacity, texture parameters, and mechanical properties, all valuable for applications in engineering land use. MIR PLS analyses showed high potential to quantify CEC, LL, PL, LS, COLE, and **W**, and modest potential for the assessment of PI and VS for an independent set. The technique showed minimal potential for the estimation of sodicity indices, activity numbers, and textural parameters for the studied soils; however, the MIR spectral predictors are accurate in discriminating soils into 'stable/unstable' categories. MIR screening could effectively sort soil properties into quality categories commonly used in materials testing with accuracy considered adequate for preliminary geotechnical investigations where only semi-quantitative or qualitative information is required to guide management decisions. Calibration models, based on separate depth sample datasets, are more robust than their mixed depth counterparts. We can conclude that MIR PLS has the potential for rapid materials testing for earthen works and small building construction, especially for preliminary screening and the assessment of for follow-up conventional analyses. Further studies should test the MIR PLS performance for a more diverse range in soil types following a spectral library approach, and the direct calibration of MIR to measure the soil functional capacity (for instance stability, permeability, strength, and workability) applied in civil engineering. As a result of this work, linear shrinkage and the Atterberg limits were subsequently

included as standard reference methods in the Africa Soil Information Service baseline sample of sub-Saharan Africa.

Abbreviations and symbols

Code	Description
A	activity number
AAS	atomic absorption spectrophotometry
AES	atomic emission spectrophotometry
AfSIS	Africa Soil Information Service
BS	British Standard
BSI	British Standards Institution
CEC	cation exchange capacity
COLE	coefficient of linear extensibility
CV	coefficient of variation
DRIFTS	diffuse reflectance infrared Fourier transform spectroscopy
eCa	exchangeable calcium
eK	exchangeable potassium
eMg	exchangeable magnesium
eNa	exchangeable sodium
ESP	exchangeable sodium percent
GIS	geographic information system
H	robust Mahalanobis distance
Hby	Homa Bay sentinel site
IR	infrared spectroscopy
KCL	potassium chloride
LDSF	land degradation surveillance framework
LHR	likelihood ratio
LL	liquid limit
ln	natural logarithm
Lny	Lower Nyando sentinel site
looCV	leave-out-one crossvalidation
LS	linear shrinkage
LVB	Lake Victoria basin
W	air-dried gravimetric moisture content
MIR	mid-infrared diffuse reflectance
Na5	Na-ion content in 1:5 soil-to-water extract
NIR	near-infrared diffuse reflectance
NP	non-plastic
OPUS	optic user's software
PC	principle component
PCA	principal component analysis
PI	plasticity index
PL	plastic limit
PLSR	partial least-square regression (PLS)
r	correlation coefficient
r^2	coefficient of determination for measured and predicted values
RMSECV	root mean square error of cross validation for calibration set
RMSEP	root mean square error of prediction for validation set
RPD	ratio of SD of reference values to RMSECV/RMSEP
SD	standard deviation for measured values
SIMCA	soft independent modeling of class analogy
SOC	soil organic carbon content
SQRT	square root
tClay	total clay content
tSa	total sand content
tSi	total silt content
VS	volumetric shrinkage

Acknowledgments

The authors gratefully acknowledge the support received by Ms Akinyi of the Materials Testing and Research Laboratory, KPC Rao at ICRAF Soil Laboratory for assistance with the wet chemistry analyses, and Elvis Weullow and the Soil and Plant Spectral Diagnostic Laboratory team at ICRAF for soil processing and spectral measurements. Thanks are also extended to the Joash Mango and ICRAF Kisumu field team for collaboration during the field work. This study was jointly funded by the Kenya Agricultural and Livestock Research Organization (KALRO), Kenya Agricultural Productivity Project (KAPP), and the World Agroforestry Centre (ICRAF) Science Domain 4 – Land Health Decisions.

References

Ben-Dor, E., Heller, D., Chudnovsky, A., 2008. A novel method of classifying soil profiles in the field using optical means. Soil Sci. Soc. Am. J. 72, 1113–1123.

British Standards Institute (BSI), 1975. Methods of Test for Soils for Civil Engineering Purposes. British Standards Institution, 2 Park Street, Landon (Chapter 2).

Brown, D.J., Bricklemyer, R.S., Miller, P.R., 2005. Validation requirements for diffuse reflectance soil characterization models with a case study of VNIR soil C prediction in Montana. Geoderma 129, 251–267.

CAMO ASA Inc., 1998. The Unscrambler User Manual. CAMO Inc., Corvallis, OR.

Canasveras, J.C., Barron, V., del Campillo, M.C., Torrent, J., Gomez, J.A., 2010. Estimation of aggregate stability indices in Mediterranean soils by diffuse reflectance spectroscopy. Geoderma 158, 78–84.

Cantarella, H., Quaggio, J.A., van Raij, B., Abreu, M.F., 2006. Variability of soil analysis of commercial laboratories: implications for lime and fertilizer recommendations. Commun. Soil Sci. Plant Anal. 37, 2213–2225.

Fratta, D., Aquettant, J., Roussel-Smith, L., 2007. Introduction to Soil Mechanics Laboratory Testing. CRC Press, Boca Raton (Chapter 3).

Gee, G.W., Bauder, J.W., 1986. Particle-size analysis. In: Klute, A. (Ed.), Methods of Soil Analysis, Part 1, Physical and Minerological Methods 2nd ed. American Society of Agronomy, Madison, WI, pp. 383–411.

Hazelton, P., Murphy, B., 2007. Interpreting Soil Test Results: What Do All The Numbers Mean?. CSIRO Publishing, Collingwood Australia31–47.

Howari, F.M., Goodell, P.C., Miyamoto, S., 2002. Spectral properties of salt crusts formed on saline soils. J. Environ. Qual. 31, 1461–1473.

Igwe, C.A., 2003. Shrink–swell potential of floodplain soils in Nigeria in relation to moisture content and mineralogy. J. Int. Agrophys. 17, 47–55.

Irvine, S.A., Reid, D.J., 2001. Field prediction of sodicity in dryland agriculture in Central Queensland. Aust. J. Soil Res. 39, 1349–1357.

Islam, K., Singh, B., McBratney, A.B., 2003. Simultaneous estimation of several soil properties by ultra-violet, visible, and near-infrared spectroscopy. Aust. J. Soil Res. 41, 1101–1114.

Janik, L.J., Merry, R.H., Skjemstad, J.O., 1998. Can mid infrared diffuse reflectance analysis replace soil extractions? A review. Aust. J. Exp. Agric. 38, 681–696.

Janik, L.J., Merry, R.H., Forrester, S.T., Lanyon, D.M., Rawson, A., 2007. Rapid prediction of soil water retention using mid infrared spectroscopy. Soil Sci. Soc. Am. J. 71, 507–514.

Kariuki, P.C., van Der Meer, F.D., 2015. A unified swelling potential index for expansive soils. Eng. Geol. (in press).

Kariuki, P.C., van Der Meer, F.D., Siderius, W., 2003. Classification of soils based on Engineering Indices and spectral data. Int. J. Remote Sens. 24, 2567–2574.

Linker, R., 2012. Application of FTIR spectroscopy to agricultural soils analysis. Fourier Transforms – New Analytical Approaches and FTIR Strategies, 385–404.

Minasny, B., McBratney, A.B., 2006. A conditioned Latin hypercube method for sampling in the presence of ancillary information. Comput. Geosci. 32, 1378–1388.

Mouazen, A.M., De Baerdemaeker, J., Ramon, H., 2006. Characterization of soil water content using measured visible and near infrared spectra. Soil Sci. Soc. Am. J 70, 1295–1302.

Naes, T., Isaksson, T., Fearn, T., Davies, T., 2002. A User-friendly Guide to Multivariate Calibration and Classification. NIR Publications, Chichester, UK.

Nanni, M.F., Demattè, J.A., 2006. Spectral reflectance methodology in comparison to traditional soil analysis. Soil Sci. Soc. Am. J 70, 393–407.

Nguyen, T.T., Janik, L.J., Raupach, M., 1991. Diffuse reflectance infrared Fourier transform (DRIFT) spectroscopy in soil studies. Aust. J. Soil Res. 29, 49–67.

Pirie, A., Singh, B., Islam, K., 2005. Ultra-violet, visible, near-infrared, and mid-infrared diffuse reflectance spectroscopic techniques to predict several soil properties. Aust. J. Soil Res. 43, 713–721.

R-Development Core Team, 2012. R: A Language and Environment for Statistical Computing. R Foundation for Statistical Computing, Vienna.

Reeves, J.B., 2010. Near-versus mid-infrared diffuse reflectance spectroscopy for soil analysis emphasizing carbon and laboratory versus on-site analysis: where are we and what needs to be done?. Geoderma 158, 3–14.

Shepherd, K.D., 2010. Soil spectral diagnostics – infrared, x-ray and laser diffraction spectroscopy for rapid soil characterization in the Africa Soil Information Service. In: Proceedings of the 19th World Congress of Soil Science, Soil Solutions for a Changing World, 1–6 August 2010, Brisbane, Australia. Published on CDROM.

Shepherd, K.D., Walsh, G.M., 2002. Development of reflectance spectral libraries for characterization of soil properties. Soil Sci. Soc. Am. J 66, 988–998.

Shepherd, K.D., Walsh, M.G., 2003. Improving accuracy and quality of routine soil analyses using diffuse reflectance spectroscopy. In: Paper presented at ASA-CSSA-SSSA Annual Meetings, 2–6 November 2003, Denver, Colorado, USA.

Shepherd, K.D., Walsh, M.G., 2007. Infrared spectroscopy – enabling an evidence-based diagnostic surveillance approach to agricultural and environmental management in developing countries. J. Near Infrared Spectrosc. 15, 1–19.

Shepherd, K.D., Vanlauwe, B., Gachengo, C.N., Palm, C.A., 2005. Decomposition and mineralization of organic residues predicted using near infrared spectroscopy. Plant Soil 277, 315–333.

Stenberg, B., 2010. Effects of soil sample pretreatments and standardized rewetting as interacted with sand classes on vis–NIR predictions of clay and soil organic carbon. Geoderma 158, 15–22.

Taylor, R., 1990. Interpretation of the correlation coefficient: a basic review. J. Diagn. Med. Sonogr. 6, 35–39.

Terhoeven-Urselmans, T., Vågen, Tor-G., Spaargaren, O., Shepherd, K.D., 2010. Prediction of soil fertility properties from a globally distributed soil mid-infrared spectral library. Soil Sci. Soc. Am. J. 74, 1792–1799.

Thomas, P.J., Baker, J.C., Zelazny, L.W., 2000. An expansive soil index for predicting shrink–swell potential. Soil Sci. Soc. Am. J 64, 268–274.

Todorov, V., 2013. Robust Multivariate Methods for High Dimensional Data. rrcovHD: R Package version 0.2-2.

Vågen, Tor-G., Winowiecki, L.A., Tondoh, J.E., Desta, L.T., 2013. Africa Soil Information Service (AfSIS) – Soil Health Mapping. http://hdl.handle.net/1902.1/19793 V2 [Version].

Viscarra Rossel, R.A., Walvoort, D.J.J., McBratney, A.B., Janik, L.J., Skjemstad, J.O., 2006. Visible, near-infrared, mid-infrared or combined diffuse reflectance spectroscopy for simultaneous assessment of various soil properties. Geoderma 131, 59–75.

Viscarra Rossel, R.A., McBratney, A.B., 1998. Soil chemical analytical accuracy and costs: implications from precision agriculture. Aust. J. Exp. Agric. 38, 765–775.

Viscarra Rossel, R.A., Jeon, Y.S., Odeh, I.O.A., McBratney, A.B., 2008. Using a legacy soil sample to develop a mid-IR spectral library. Aust. J. Soil Res. 46, 1–16.

Wang, Y., Cao, Z., 2013. Expanded reliability-based design of piles in spatially variable soil using efficient Monte Carlo simulations. Soils Found. 53, 820–834.

Waruru, B.K., Shepherd, K.D., Ndegwa, G.M., Kamoni, P.T., Sila, A., 2014. Rapid estimation of soil engineering properties using diffuse reflectance near infrared spectroscopy. Biosyst. Eng. 121, 177–185.